Inorg. Chem. **2008**, *47*, 2987−2993

Species Distribution and Coordination of Uranyl Chloro Complexes in Acetonitrile

Christoph Hennig,*,† Kelly Servaes,‡ Peter Nockemann,‡ Kristof Van Hecke,‡ Luc Van Meervelt,‡ Johan Wouters,§ Linda Fluyt,‡ Christiane Görller-Walrand,‡ and Rik Van Deun‡

Institute of Radiochemistry, Forschungszentrum Dresden-Rossendorf, P.O. Box 510119, D-01314 Dresden, Germany, Department of Chemistry, Katholieke Universiteit Leuven, Celestijnenlaan 200F, B-3001 Leuven, Belgium, and Laboratoire de Chimie Biologique Structurale, FUNDP - Fac. des Sciences, 61 Rue de Bruxelles, B-5000 Namur, Belgium

Received July 20, 2007

The complex formation of the uranyl ion, UO_2^{2+}, with chloride ions in acetonitrile has been investigated by factor analysis of UV–vis absorption and U L_3 edge EXAFS (extended X-ray absorption fine structure) spectra. As a function of increasing $[Cl^-]/[UO_2^{2+}]$ ratio, the five monomeric species $[UO_2(H_2O)_5]^{2+}$, $[UO_2Cl(H_2O)_2(MeCN)_2]^+$, $[UO_2Cl_2(H_2O)(MeCN)_2]$, $[UO_2Cl_3(MeCN)_2]^-$, and $[UO_2Cl_4]^{2-}$ have been observed. The distances determined in the first coordination sphere are: $U-O_{ax} = 1.77$ Å, $U-O_{H2O} = 2.43$ Å, $U-N_{MeCN} = 2.53$ Å, and $U-Cl = 2.68$ Å. A crystalline material has been obtained from the intermediate solution with the $[Cl^-]/[UO_2^{2+}]$ ratio of ∼2, where $[UO_2Cl_2(H_2O)(MeCN)_2]$ is the dominating species. The crystal structure analysis of this material revealed a tetrameric complex, $[(UO_2)_4(\mu_2\text{-}Cl)_4(\mu_3\text{-}O)_2(H_2O)_2(CH_3CN)_4]\cdot(CH_3CN)$. The crystal data are: monoclinic, space group $P2_1/n$, $a = 10.6388(5)$ Å, $b = 14.8441(5)$ Å, $c = 10.8521(5)$ Å, $\beta = 109.164(5)°$, and $Z = 2$. The U(VI) coordination of the solution species $[UO_2Cl_2(H_2O)(MeCN)_2]$ changes during the crystallization by replacing one MeCN molecule with a bridging μ_3-O atom in the tetramer.

Introduction

Chloride coordination alters the stability of actinide complexes in solution. The solubility of actinides in highly concentrated chloride solutions is about 1 order of magnitude higher than in solutions with noncoordinating electrolytes.[1] Nevertheless, the chloride anion in aqueous solution is a weak ligand for UO_2^{2+} which is reflected by the fact that only two stability constants are reported in the actual Nuclear Energy Agency (NEA) thermodynamic database; $\log \beta_1^0 = 0.17 \pm 0.02$ and $\log \beta_2^0 = -1.1 \pm 0.02$ for the reaction $UO_2^{2+} + nCl^- \rightleftharpoons UO_2Cl_n^{2-n}$.[2] The safety assessment of nuclear waste disposal in geological salt formations, for example, the Waste Isolation Pilot Plant (U.S.A.) and the Gorleben test site (Germany), raises the question of chloride speciation in highly concentrated chloride solutions because of the possible migration through concerned aquifers. In contrast to aqueous solutions, the chloride anion forms with U(VI) strong complexes in organic solvents. Such chloro complexes in ionic liquids may have some importance for the reprocessing by partitioning and further transmutation of highly radioactive waste.[3] Several experimental and theoretical attempts have been made to reveal U(VI) chloro complexes with higher coordination numbers than those provided in the thermodynamic database.[4–7] In aqueous solution up to three U(VI) chloro complexes, $[UO_2Cl]^+$, $[UO_2Cl_2]^0$, and $[UO_2Cl_3]^-$, have been observed by EXAFS (extended X-ray absorption fine structure) and UV–vis spectroscopy.[7–9] Nguyen-

* To whom correspondence should be addressed. E-mail: hennig@esrf.fr.
† Forschungszentrum Dresden-Rossendorf.
‡ Katholieke Universiteit Leuven.
§ FUNDP - Fac. des Sciences.

(1) Runde, W.; Neu, M. P.; Conradson, S. D.; Clark, D. L.; Palmer, P. D.; Reilly, S. D.; Scott, B. L.; Tait, C. D. *Mater. Res. Soc. Symp. Proc.* **1997**, *465*, 693.
(2) Guillaumont, R.; Fanghänel, T.; Fuger, J.; Grenthe, I.; Neck, V.; Palmer, D. A.; Rand, M. H. *Update on the chemical thermodynamics of uranium, neptunium, plutonium, americium and technetium*; Elsevier Science Publishers: Amsterdam, 2003.
(3) Gaillard, C.; Chaumont, A.; Billard, I.; Hennig, C.; Ouadi, A.; Wipff, G. *Inorg. Chem.* **2007**, *46*, 4815.
(4) Servaes, K.; Hennig, C.; Van Deun, R.; Görller-Walrand, C. *Inorg. Chem.* **2005**, *44*, 705.
(5) Soga, T. *Spectrochim. Acta* **2000**, *56*, 79.
(6) Van Besien, E.; Pierloot, K.; Görller-Walrand, C. *Phys. Chem. Chem. Phys.* **2006**, *8*, 4311.
(7) Allen, P. G.; Bucher, J. J.; Shuh, D. K.; Edelstein, N. M.; Reich, T. *Inorg. Chem.* **1997**, *36*, 4676.
(8) Paviet-Hartmann, P.; Lin, M. R. *Mater. Res. Soc. Symp. Proc.* **1999**, *556*, 977.

10.1021/ic7014435 CCC: $40.75
Published on Web 03/14/2008

Trung et al. indentified the species $[UO_2Cl]^+$, $[UO_2Cl_2]^0$, $[UO_2Cl]^{3-}$, $[UO_2Cl_4]^{2-}$, and $[UO_2Cl_5]^{3-}$ with Raman spectroscopy.[3–10] However, according to the authors knowledge, the pentachloro species has not been confirmed yet by other methods. The actual known crystal structure and spectroscopic data of solids and solution species suggest the $UO_2Cl_4^{2-}$ unit as the limiting species.[4,11,12] In contrast, the pentacoordinated complex $UO_2F_5^{3-}$ has been observed under different conditions.[13,14] $[UO_2Cl_4]^{2-}$ has the centrosymmetric symmetry D_{4h} which is related with a characteristic vibronic UV–vis spectrum.[4,11,15,16] The UV–vis absorption spectrum of the limiting species $[UO_2Cl_4]^{2-}$ is well understood, but structural details of the intermediate species are still under discussion. Paviet-Hartmann and Lin extracted the quantitative species distribution of $[UO_2]^{2+}$, $[UO_2Cl]^+$, and $[UO_2Cl_2]^0$ in aqueous solution by principal component analysis of UV–vis spectra.[8] However, at present, the analysis of the full U(VI) chloride species distribution including the limiting species $UO_2Cl_4^{2-}$ is missing in the literature.

The aim of this study is to correlate the species distribution and the coordination of uranyl chloro complexes by combining UV–vis and EXAFS spectroscopy. The UV–vis spectra of UO_2^{2+} arise from electronic transitions $(\sigma_u^+)^2 \rightarrow \sigma_u^+\delta_u$ and $(\sigma_u^+)^2 \rightarrow \sigma_u^+\varphi_u$.[17] Because both orbitals have 5f character, the observed f−f transition is Laporte forbidden, and the UV–vis absorption spectra show typical vibronic features. These vibrations occur either by the static ligand field interactions or by the vibronic coupling and are sensitive to arrangement and type of ligands. The typical vibrational fine structure in UV–vis spectra of UO_2^{2+} ions is affected by the symmetry of the first coordination sphere, whereas the chemical nature of the ligands has an influence on the frequency of the symmetrical stretching vibration ν_s of the trans-dioxo atoms.[18] If the coordination mode and symmetry of the individual species are sufficiently different from each other, the UV–vis spectra can be correlated with the individual species in the solution. The task to extract the individual spectra from a sample series with different coexisting species can be solved by factor analysis (or principal component analysis) including a target transformation.[19] EXAFS spectra contain information on the distances R_i and coordination numbers N_i of the first coordination shells. Because of differences in R_i, several backscattering atoms can be separated from each other by factor analysis. It has been shown that factor analysis is able to reveal the species distribution from a series of UV–vis absorption spectra[8,20] and is also able to extract the main interatomic distances from EXAFS.[9,21–23] UV–vis absorption spectroscopy and EXAFS are both especially sensitive in the same concentration range of U(VI) in solution.

Experimental Section

Sample Preparation. $UO_2(ClO_4)_2 \cdot 6H_2O$ was mixed with tetrabutylammonium chloride in acetonitrile to obtain 50 mM UO_2^{2+} and $[UO_2^{2+}]/[Cl^-]$ ratios ranging from 1:0 to 1:4 in concentration steps of 0.2. The starting material $UO_2(ClO_4)_2 \cdot 6H_2O$ was prepared by dissolving UO_3 (Lachema) in 2 M perchloric acid. The solution was boiled to expel free chlorine. After dilution with water, the solution was subsequently evaporated to close to dryness. This procedure was repeated until white fumes disappeared. Finally, a yellow powder of $UO_2(ClO_4)_2 \cdot 6H_2O$ was obtained.[24] Tetrabutylammonium chloride was purchased from Fluka. Extra dry acetonitrile with less than 50 ppm water, dried on molecular sieves, was purchased from Acros.

UV–vis Absorption Measurements. UV–vis absorption spectra were recorded at room temperature with a Varian Cary 5000 spectrophotometer between 600 and 300 nm. The spectra were collected in quartz cuvettes (optical path length 10 mm). The UV–vis data have been analyzed by factor analysis using the program ITFA.[21]

EXAFS Measurements. EXAFS measurements were carried out at the Rossendorf Beamline[25] at the European Synchrotron Radiation Facility. The monochromator, equipped with a Si(111) double-crystal, was used in channel-cut mode. Higher harmonics were rejected by two Pt coated mirrors. All experiments were performed at room temperature. The spectra of the solutions were collected in transmission mode using argon-filled ionization chambers, and the solid sample was measured in fluorescence mode with a 13-element detector. The monochromator energy scale was calibrated to the K edge of an Y metal foil (first inflection point assigned to 17038 eV). The EXAFS oscillations were extracted from the raw absorption spectra by standard methods including a μ_0 spline approximation for the atomic background using the WINXAS[26] and the EXAFSPAK[27] software packages. EXAFS analysis was complemented by factor analysis using the program ITFA.[21] The data analysis has been performed in three steps: (i) decomposition

(9) Hennig, C.; Tutschku, J.; Rossberg, A.; Bernhard, G.; Scheinost, A. C. *Inorg. Chem.* **2005**, *44*, 6655.
(10) Nguyen-Trung, C.; Begun, G. M.; Palmer, D. A. *Inorg. Chem.* **1992**, *31*, 5280.
(11) Görller-Walrand, C.; De Houwer, S.; Fluyt, L.; Binnemans, K. *Phys. Chem. Chem. Phys.* **2004**, *6*, 3292.
(12) Inorganic Crystal Structure Database, Version October 2007, Fachinformationzentrum Karlsruhe.
(13) Luchev, A. A.; Mashriov, K. G.; Smolin, Y. I.; Shepelev, Y. F. *Radiokhimiya* **1986**, *28*, 628.
(14) Vallet, V.; Wahlgren, U.; Schimmelpfennig, B.; Moll, H.; Szabó, Z.; Grenthe, I. *Inorg. Chem.* **2001**, *40*, 3516.
(15) (a) Tanner, P. A. *J. Chem. Soc., Faraday Trans.* **1984**, *80*, 365. (b) Flint, C. D.; Tanner, P. A. *Mol. Phys.* **1981**, *44*, 411. (c) Flint, C. D.; Tanner, P. A. *J. Chem. Soc., Faraday. Trans.* **1981**, *77*, 1865.
(16) Denning, R. G.; Snellgrove, T. R.; Woodwark, D. R. *Mol. Phys.* **1979**, *37*, 1109.
(17) Denning, R. *J. Phys. Chem. A* **2007**, *111*, 4125.
(18) Görller-Walrand, C.; De Jaegere, S. *Spectrochim. Acta, Part A* **1972**, *28*, 257.
(19) Malinowski, E. R. *Factor analysis in chemistry*; John Wiley & Sons: New York, 1991.
(20) Meinrath, G.; Lis, S.; Glatty, Z. *J. Chem. Thermodyn.* **2006**, *38*, 1274.
(21) Rossberg, A.; Reich, T.; Bernhard, G. *Anal. Bioanal. Chem.* **2003**, *376*, 631.
(22) Jalilehvand, F.; Mah, V.; Leung, B. O.; Ross, D.; Parvez, M.; Aroca, R. *Inorg. Chem.* **2007**, *46*, 4430.
(23) Wasserman, S. R.; Allen, P. G.; Shuh, D. K.; Bucher, J. J.; Edelstein, N. M. *J. Synchrotron Radiat.* **1999**, *6*, 284.
(24) Various hydrates of uranyl perchlorate have been reported. In this study, we use the molecular weight of the hexahydrate for calculating concentrations (MW 577.02 g/mol). The uncertainty of the water content may introduce a small deviation from stoichiometry.
(25) Matz, W.; Schell, N.; Bernhard, G.; Prokert, F.; Reich, T.; Claussner, J.; Oehme, W.; Schlenk, R.; Dienel, S.; Funke, H.; Eichhorn, F.; Betzl, M.; Prohl, D.; Strauch, U.; Huttig, G.; Krug, H.; Neumann, W.; Brendler, V.; Reichel, P.; Denecke, M. A.; Nitsche, H. *J. Synchr. Radiat.* **1999**, *6*, 1076.
(26) Ressler, T. *J. Synchr. Radiat.* **1998**, *5*, 118.
(27) George, G. N.; Pickering, I. J. *EXAFSPAK, a suite of computer programs for analysis of X-ray absorption spectra*; Stanford Synchrotron Radiation Laboratory: Menlo Park, CA, 2000.

of the experimental spectra into principal components (abstract spectra) by factor analysis, (ii) transformation of the principal components into real spectra by iterative target transformation, and (iii) standard shell fitting of the real spectra to gain structural parameters of the limiting structural units. Standard shell fitting has been performed by using theoretical phase and amplitude functions calculated with the FEFF 8.2 code.[28] The scattering interactions were calculated using $UO_2Cl_2(H_2O)(MeCN)_2 \cdot 2MeCN$[29] and $Cs_2UO_2Cl_4$.[30] The multiple scattering path between uranium and the axial arranged trans-dioxo atoms (O_{ax}), was included in the curve fit by constraining its Debye–Waller factor and its effective path length to twice the values of the corresponding, freely fitted U−O_{ax} single-scattering path. The amplitude reduction factor, S_0^2, was defined as 0.9 in the FEFF calculation and fixed to that value in the data fits.

Crystallographic Data. Single crystals of $[(UO_2)_4(\mu_2\text{-}Cl)_4(\mu_3\text{-}O)_2(H_2O)_2(CH_3CN)_4] \cdot (CH_3CN)$ have been crystallized from an acetonitrile solution with a $[Cl^-]/[UO_2^{2+}]$ ratio of ∼2 in a sealed polyethylene vessel after 10 days. Empirical formula: $C_{12}H_{18}Cl_4N_6O_{12}U_4$, M = 1532.24 g mol^{-1}, monoclinic, $P2_1/n$ (No. 14), a = 10.6388(5) Å, b = 14.8441(5) Å, c = 10.8521(5) Å, β = 109.164(5)°, V = 1618.83(13) Å^3, T = 100(2) K, Z = 2, ρ_{calc} = 3.144 g cm^{-3}, μ(Mo Kα) = 20.33 mm^{-1}, $F(000)$ = 1328, crystal size 0.4 × 0.4 × 0.4 mm, and 3294 independent reflections (R_{int} = 0.0589). Final R = 0.0440 for 2942 reflections with $I > 2\sigma(I)$ and $\omega R2$ = 0.1266 for all data. Intensity data were collected on a Gemini R Ultra diffractometer equipped with CCD detector using Mo Kα radiation (λ = 0.71073 Å). The images were interpreted and integrated with the program CrysAlisPro from Oxford Diffraction.[31] The structure was solved by direct methods and refined by full-matrix least-squares on F^2 using the SHELXTL program package.[32] Nonhydrogen atoms were anisotropically refined, and the hydrogen atoms in the riding mode with isotropic temperature factors fixed at 1.5 times for the methyl groups. CCDC-679899 contains the supplementary crystallographic data for this paper and can be obtained free of charge via www.ccdc.cam.ac.uk/products/csd/request/ (or from the Cambridge Crystallographic Data Centre, 12, Union Road, Cambridge CB2 1EZ, UK; fax: +44–1223–336033; or deposit@ccdc.cam.ac.uk).

Results and Discussion

The UV–vis absorption spectra of a sample series with 50 mM U(VI) in MeCN in the presence of an increasing amount of Cl^- in the range of 0−210 mM are plotted in Figure 1.

The spectrum at the bottom of Figure 1, containing the pure solvated ion, $[UO_2(solv)_n]^{2+}$, shows weak absorption bands. The nature of this solvated species will be discussed later by using the results from EXAFS measurements. With increasing $[Cl^-]/[UO_2^{2+}]$ ratio, the peak positions and intensities change stepwise but remain then unchanged above 180 mM Cl^-. The spectral features of the samples with high $[Cl^-]$ exhibit a significant vibrational fine structure indicating the centrosymmetric complex $[UO_2Cl_4]^{2-}$ with D_{4h} symmetry. This spectrum has been analyzed in detail elsewhere.[4,16] The intermediate species show

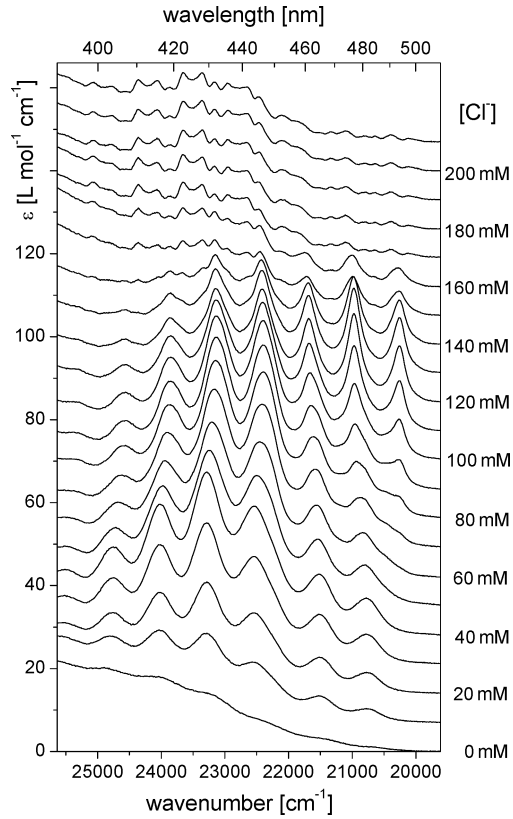

Figure 1. UV–vis absorption spectra of 50 mM UO_2^{2+} with increasing amount of Cl^- in acetonitrile at room temperature.

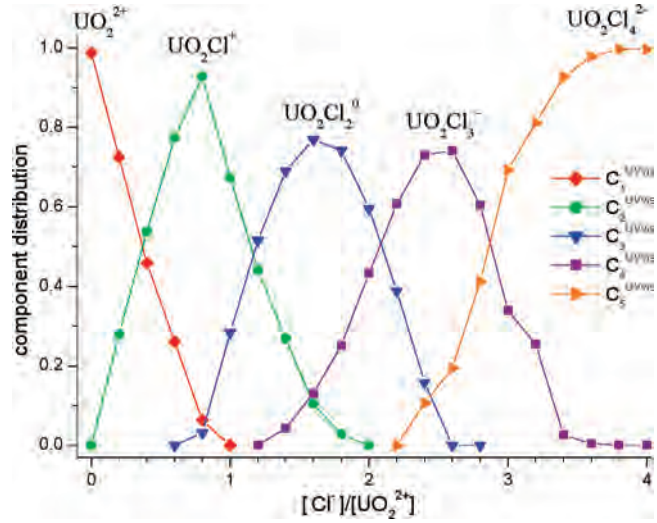

Figure 2. Component distribution revealed from the UV–vis absorption spectra. The components represent the individual solution species.

strong resonance intensities especially in the low wavenumber region. Only the first and the last spectrum of the series represent pure solution species, whereas it can be assumed that the intermediate species do occur as mixtures but not in a pure state. The spectra of the intermediate species, as well as the quantitative species distribution, have been extracted by factor analysis as a function of the $[Cl^-]/[UO_2^{2+}]$ ratio. There are five principal components (C_1^{UVvis}−C_5^{UVvis}) which have been obtained from the experimental spectra. The species distribution from the UV–vis absorption spectra is shown in Figure 2.

(28) Rehr, J. J.; Albers, R. C. *Rev. Mod. Phys.* **2000**, *72*, 621.
(29) Hall, T. J.; Mertz, C. J.; Bachrach, S. M.; Hipple, W. G.; Rogers, R. D. *J. Crystallogr. Spectrosc. Res.* **1989**, *19*, 499.
(30) WatkinD. J.; Denning, R. G.; Prout, K. *Acta Crystallogr.* **1991**, *C47*, 2517.
(31) Oxford Diffraction. *ABSPACK and CrysAlisPro.*; Oxford Diffraction Ltd: Oxford, 2006.
(32) *SHELXTL-PC*, Version 5.1; Bruker Analytical X-ray Systems Inc.: Madison, WI, 1997.

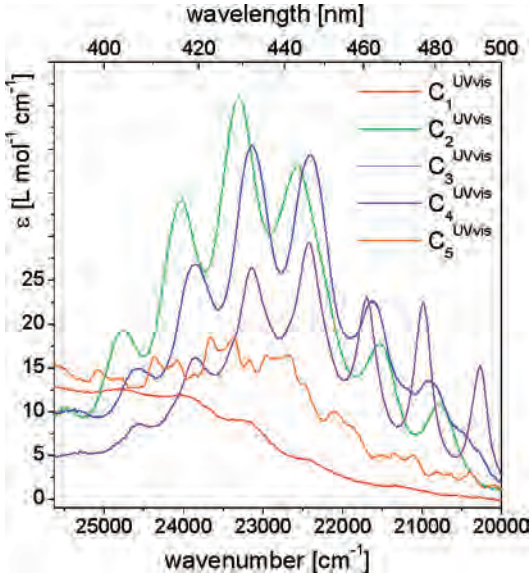

Figure 3. UV–vis spectra extracted with target transformation from the five principal components C_1^{UVvis}, $[UO_2]^{2+}$; C_2^{UVvis}, $[UO_2Cl]^+$; C_3^{UVvis}, $[UO_2Cl_2]^0$; C_4^{UVvis}, $[UO_2Cl_3]^-$; and C_5^{UVvis}, $[UO_2Cl_4]^{2-}$.

Between the two limiting solvated species $[UO_2(solv)_n]^{2+}$, represented by C_1^{UVvis}, and the fully coordinated $[UO_2Cl_4]^{2-}$, represented by C_5^{UVvis}, there occur three further maxima in the component distribution function. Although the UV–vis spectra are sensitive to changes in the coordination, it is usually difficult to estimate the coordination itself from the spectral features. However, because of the clear correlation with the $[Cl^-]/[UO_2^{2+}]$ ratio, these maxima can be assigned to the intermediate species $[UO_2Cl]^+$, $[UO_2Cl_2]^0$, and $[UO_2Cl_3]^-$.[33] The corresponding UV–vis spectra, obtained from target transformation, are shown in Figure 3.

The pure solvated uranyl ion, $[UO_2(solv)_n]^{2+}$, exhibits an absorption spectrum with a weak vibrational fine structure between 30 000 and 18 000 cm^{-1}. The fully coordinated ion, $[UO_2Cl_4]^{2-}$, has the centrosymmetric coordination symmetry D_{4h} that originates purely vibronic resonances induced by coupling of vibrations with ungerade symmetry. The symmetric stretching vibration ν_s (a_{1g}) of the uranyl ion itself is superimposed on each vibronic transition. Besides this gerade vibration, three ungerade, intensity inducing vibrations are coupled to the electronic transitions, that is, the asymmetric stretching vibration ν_a (a_{2u}) and the bending vibration ν_b (e_u) of the axial oxygens of the uranyl ion and mainly one vibration of the equatorial ligands, ν_{10} (b_{1u}).[4,16] For the intermediate species $[UO_2Cl]^+$, $[UO_2Cl_2]^0$, and $[UO_2Cl_3]^-$, the resonances are remarkably more intense than those of the limiting species. These intense peaks have been interpreted, for example, to be due to the presence of $[UO_2Cl_3]^-$ with a noncentrosymmetric point group of D_{3h} symmetry. The corresponding spectrum has indeed some similarities, for example, with that of the trigonal $[UO_2(NO_3)_3]^-$ complex,[34] but the magnetic circular dichroism measurement of

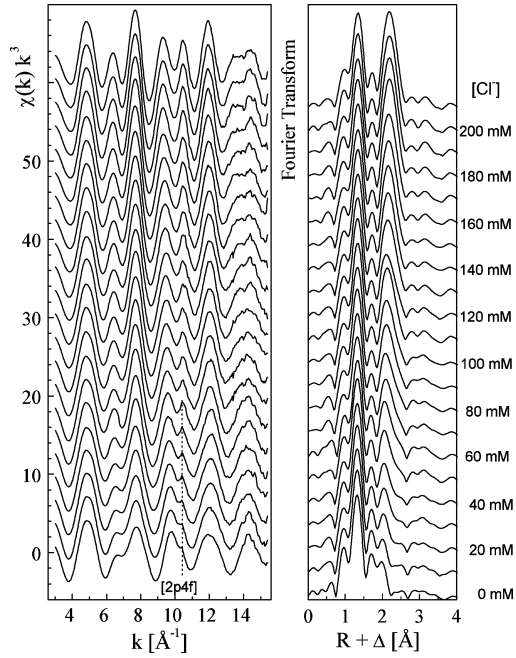

Figure 4. U L_3 edge k^3 weighted EXAFS (left) and their FT (right) of 50 mM UO_2^{2+} with increasing amount of Cl^- in acetonitrile. The [2p4f] double-electron excitation[36] is indicated by a dotted line.

this species revealed a completely different spectrum than that of the uranyl ion in D_{3h} symmetry.[11] This indicates that the interpretation of the intermediate species has actually some uncertainties.[6] Therefore, EXAFS measurements have been performed on the same sample series to gain further information on the complex coordination. The EXAFS spectra, taken from the U L_3 edge, are shown together with their Fourier transform (FT) in Figure 4. These spectra show a systematic change as function of the $[Cl^-]/[UO_2^{2+}]$ ratio. This concerns mainly the equatorial coordination shell, depicted in the FT in the distance of $R + \Delta = 1.5$ to 2.5 Å. The FT peak at $R + \Delta \sim 1.3$ Å, representing the two axial oxygen atoms of the UO_2^{2+} unit, remains unchanged. However, the differences between the spectra from one sample to the next one are relatively weak. Because in the case of such small changes factor analysis is especially sensitive to experimental noise, the upper limit of the k range has been restricted to 15.3 $Å^{-1}$ where the spectrum has an appropriate signal-to-noise ratio. The factor analysis reveals three principal components (C_1^{EXAFS}–C_3^{EXAFS}). It is difficult to interpret a priori the structural meaning of the principal components. Therefore, the EXAFS spectra which correspond to the components C_1^{EXAFS}, C_2^{EXAFS}, and C_3^{EXAFS} have been extracted by target transformation for an analysis of the structural parameters. There is a small effect from a [2p4f] double-electron excitation,[36] which is not of importance for this study. The data of the three extracted EXAFS spectra and the fit results are shown in Figure 5 and Table 1.

All three spectra show the two oxo atoms at a distance of 1.76–1.77 Å. The U–O distance of the uranyl unit UO_2^{2+}

(33) All maxima occur systematically at lower $[Cl^-]/[UO_2^{2+}]$ ratio than the expected stoichiometric ratio due to an uncertainty of the water content in the starting material.

(34) Servaes, K.; Hennig, C.; Billard, I.; Gaillard, C.; Binnemans, K.; Görrler-Walrand, C.; Van Deun, R. *Eur. J. Inorg. Chem.* **2007**, 5120.

(35) Sémon, L.; Boehme, C.; Billard, I.; Hennig, C.; Lützenkirchen, K.; Reich, T.; Rossberg, A.; Rossini, I.; Wipff, G. *ChemPhysChem* **2001**, *2*, 591.

(36) Hennig, C. *Phys. Rev. B* **2007**, *75*, 035120.

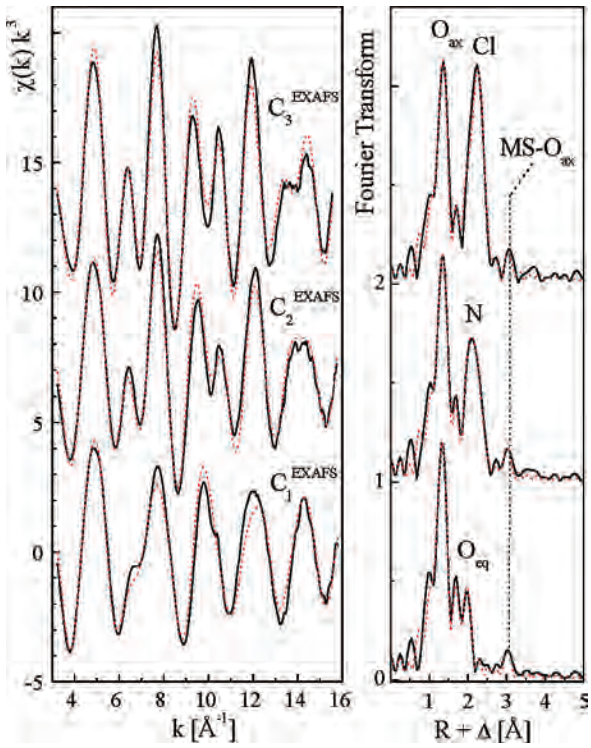

Figure 5. U L_3 edge k^3 weighted EXAFS data (left) and their corresponding FTs (right) obtained from $C_1^{EXAFS}-C_3^{EXAFS}$.

Table 1. EXAFS Parameters of the Three Principal Components of the Solution Series[a,b]

		R [Å]	N	σ^2 [Å^2]	$\Delta E_{k=0}$	F
C_3^{EXAFS}	U−O_{ax}	1.77	2.2	0.0017	1.2	0.11
	U−Cl	2.68	3.9	0.0039		
C_2^{EXAFS}	U−O_{ax}	1.77	1.9	0.0014	5.8	0.23
	U−N	2.53	4.9	0.0034		
C_1^{EXAFS}	U−O_{ax}	1.76	2.2	0.0018	2.1	0.21
	U−O_{eq}	2.43	4.7	0.0094		

[a] O_{ax}, axial oxygen (trans-dioxo group); O_{eq}, equatorial oxygen. [b] Errors in distances R are ±0.02 Å; errors in coordination numbers N are ±15%. The overall goodness of the fits, F, is given by χ^2, weighted by the magnitude of data. The threshold energy, $E_{k=0}$, was arbitrarily defined at 17185 eV and varied as a global fit parameter resulting in the energy shift $\Delta E_{k=0}$.

is invariant in this sample series. Whereas the O_{ax} scattering contribution is an unchanged part of all extracted EXAFS spectra, changes occur in the equatorial shell. It is obvious, that C_1^{EXAFS} represents the structural characteristics of the solvated species $[UO_2(solv)_n]^{2+}$; C_3^{EXAFS}, the structure of $[UO_2Cl_4]^{2-}$. To interpret the FT peaks in the equatorial position, appropriate amplitude and phase functions, $F_j(k)$ and $\varphi_{ij}(k)$, are required from a reference compound with known structure. As the coordinating ligands may be Cl^-, the solvent MeCN, and the remaining H_2O, the crystal structure of the monomer $UO_2Cl_2(H_2O)(MeCN)_2\cdot 2MeCN$, described by Hall et al.[29] is an appropriate reference for the solution species under discussion because it comprises all relevant ligands within the first coordination sphere. The average distances in the equatorial plane of this structure are U−O_{H2O} = 2.42 Å, U−N_{MeCN} = 2.53 Å, and U−Cl = 2.66 Å. Although it is usually not possible to distinguish O and N in an EXAFS fit because of its close Z number and therefore similar amplitude and phase functions, the distance difference of ∼0.1 Å between U−O_{H2O} and U−N_{MeCN} is

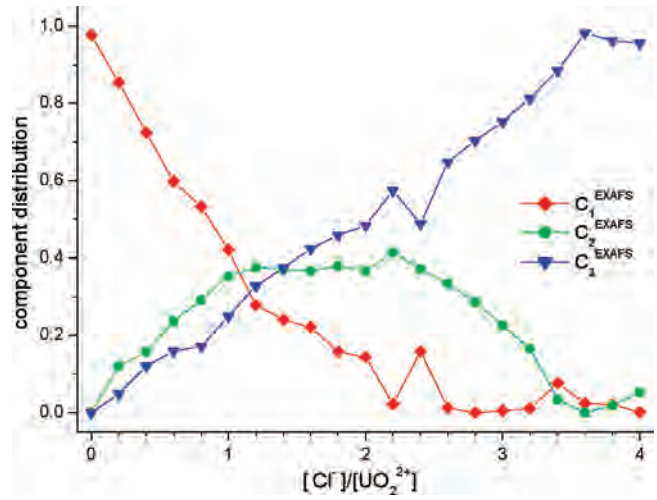

Figure 6. Component distribution revealed from the EXAFS spectra. The components represent main distances. The principal components represent the following distances in the equatorial shell: C_1^{EXAFS}, U−O; C_2^{EXAFS}, U−N; and C_3^{EXAFS}, U−Cl.

outside of the ±0.02 Å error limit of the EXAFS distance determination. An analysis of the data indicates that the spectra of the components C_1^{EXAFS}, C_2^{EXAFS}, and C_3^{EXAFS} correspond with the three scattering pairs U−O, U−N, and U−Cl (Table 1). The data fit for the pure solvated uranyl ion, $[UO_2(solv)_n]^{2+}$, revealed from C_1^{EXAFS}, indicates five equatorial oxygen atoms at a distance of 2.43 Å, which is in line with the species $[UO_2(H_2O)_5]^{2+}$. The ClO_4^- ions, present in this sample, are too weak ligands to form complexes with UO_2^{2+}.[35] The starting material, $UO_2(ClO_4)_2\cdot 6H_2O$, provides sufficient water molecules for this coordination. The observed U−O distance is in agreement with the U−O_{H2O} distance of the water molecule in the reference compound $UO_2Cl_2(H_2O)(MeCN)_2\cdot 2MeCN$.[29] Furthermore, it is close to the U−O_{H2O} distance of $[UO_2(H_2O)_5]^{2+}$ in aqueous perchlorate media, which has been determined to be 2.41 Å with EXAFS spectroscopy.[37] The Debye–Waller factor of the equatorial oxygen atoms of $[UO_2(H_2O)_5]^{2+}$ in acetonitrile is 0.0094 Å^2. This value is slightly higher than the Debye–Waller factor of $[UO_2(H_2O)_5]^{2+}$ in aqueous solution, which has been determined to be 0.0071Å^2.[37] The larger Debye–Waller factor of the equatorial shell may indicate to a minor extent an ion exchange of H_2O against MeCN, but this is not reflected by the average bond length. We can conclude that water is a relatively strong ligand in acetonitrile. The analysis of the spectrum of C_2^{EXAFS} indicates five nitrogen atoms at a distance of 2.53 Å. This distance is in good agreement with the U−N_{MeCN} distance in the crystal structure of $UO_2Cl_2(H_2O)(MeCN)_2\cdot 2MeCN$. The distribution function of the extracted distances as a function of the $[Cl^-]/[UO_2^{2+}]$ ratio is shown in Figure 6.

The component C_3^{EXAFS}, representing the U−Cl distances, shows that there is a continuous increase of the scattering

(37) Hennig, C.; Schmeide, K.; Brendler, V.; Moll, H.; Tsushima, S.; Scheinost, A. *Inorg. Chem.* **2007**, *46*, 5882.
(38) Hennig, C.; Reck, G.; Reich, T.; Rossberg, A.; Kraus, W.; Sieler, J. *Z. Kristallogr.* **2003**, *218*, 37.
(39) Palmer, D. A.; Nguyen-Trung, C. *J. Solution Chem.* **1995**, *24*, 1281.
(40) Eliet, V.; Bidoglio, G.; Omenetto, N.; Parma, L.; Grenthe, I. *J. Chem. Soc., Faraday Trans.* **1995**, *91*, 2275.

Scheme 1

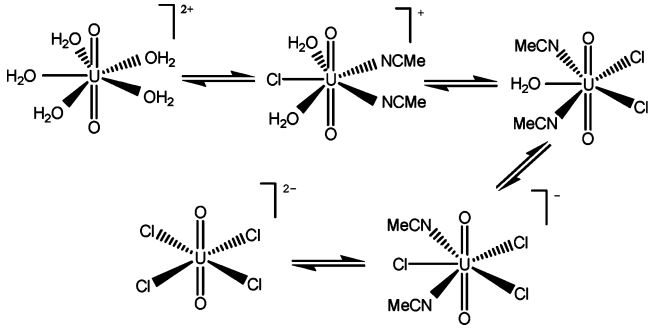

Scheme 2

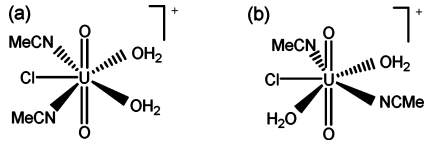

signal with increasing $[Cl^-]/[UO_2^{2+}]$ ratio. This function indicates the driving force of the Cl^- to coordinate to UO_2^{2+}. The spectrum of component C_3^{EXAFS} shows four Cl atoms at a U−Cl distance of 2.68 Å. This distance has already been reported for $[UO_2Cl_4]^{2-}$ from EXAFS measurements.[4] The component C_1^{EXAFS}, which represents the U−O scattering contribution, decreases faster with increasing $[Cl^-]/[UO_2^{2+}]$ ratio. It is partly replaced by C_2^{EXAFS}, representing the U−N bond from MeCN. The U−N bond is present in the intermediate species $[UO_2Cl]^+$, $[UO_2Cl_2]^0$, and $[UO_2Cl_3]^-$ but obviously not in the pure solvated ion $[UO_2(H_2O)_5]^{2+}$. However, as shown in Figure 6, there is no $[Cl^-]/[UO_2^{2+}]$ ratio where C_2^{EXAFS} reaches a unique presence in the distribution diagram. The spectrum of the principal component C_2^{EXAFS} represents therefore the extrapolation to the hypothetical limiting complex $[UO_2(MeCN)_5]^{2+}$. The distribution function of C_2^{EXAFS} is normalized to the coordination of this limiting complex. It is thus obvious, that the three intermediate species $[UO_2Cl]^+$, $[UO_2Cl_2]^0$, and $[UO_2Cl_3]^-$, contain each two coordinated MeCN ions. Accordingly, the numbers of coordinating H_2O molecules have been derived in relation to $[UO_2(H_2O)_5]^{2+}$ as the limiting species. In conclusion, five species have been observed: $[UO_2(H_2O)_5]^{2+}$, $[UO_2Cl(H_2O)_2(MeCN)_2]^+$, $[UO_2Cl_2(H_2O)(MeCN)_2]$, $[UO_2Cl_3(MeCN)_2]^-$, and $[UO_2Cl_4]^{2-}$. The coordination of these species is summarized in Scheme 1.

The EXAFS spectra reveal the number of coordinating ligands but not their spatial arrangement in the equatorial plane. We therefore have to consider other isomers for the intermediate species than those proposed in Scheme 1. As an example, two possible isomers for $[UO_2Cl]^+$ are shown in Scheme 2. These isomers may differ from each other in the spatial arrangement of their ligands. This point could be clarified, for example, if a solution species could be preserved in a crystal structure. From the solution with a $[Cl^-]/[UO_2^{2+}]$ ratio of ~2, we obtained a crystalline precipitate. The EXAFS spectrum of the precipitate is shown in Figure 7. This spectrum was obtained in fluorescence mode from some crystals with a size <0.4 mm. It shows significant U−U interactions between 3.6 and 3.9 Å, indicating a polynuclear or polymeric structure as a consequence of ligand

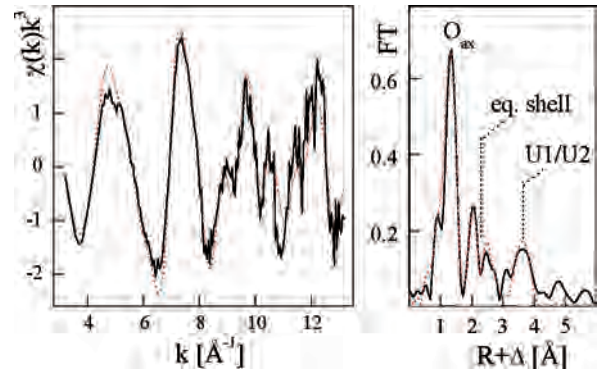

Figure 7. U L_3 edge k^3 weighted EXAFS data (left) of the precipitated crystals and their corresponding FTs (right). Distances and coordination numbers were taken from the crystal structure and kept fixed during the shell fit. The obtained Debye–Waller factors are O_{ax}, 0.0055 Å^2; O_μ, 0.012 Å^2; O_{H2O}, 0.014 Å^2; N_{MeCN}, 0.0031 Å^2; Cl, 0.011 Å^2; U1, 0.0035 Å^2; U2, 0.0055 Å^2; and weighted F-value, 0.34.

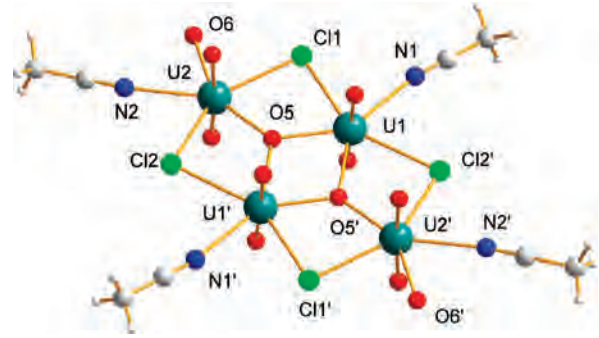

Figure 8. Molecular structure of the tetramer $[(UO_2)_4(\mu_2\text{-}Cl)_4(\mu_3\text{-}O)_2(H_2O)_2(CH_3CN)_4]\cdot(CH_3CN)$. The noncoordinating acetonitrile molecule is omitted for clarity.

rearrangement during the crystallization. The FT peaks representing the equatorial shell are different from those of the corresponding solution species. The relative low peak intensity originates obviously from the superposition of several different scattering contributions. A free fit without knowledge of the crystal structure was not successful. Therefore, the shell fit shown in Figure 7 was performed using the bond lengths and the coordination numbers from single crystal structure data given in the next section. Distances and coordination numbers were fixed in the shell fit. The obtained Debye–Waller factors, σ^2, which comprise the contributions from structural disorder as well as from thermal vibration, are given in the caption of Figure 7.

A comparison of the EXAFS from the solution species and the solid structure indicates, that the tetramer has a low stability in solution and occurs therefore as a precipitate. This is in line with the solubility of other U(VI) polymers.[2]

The same crystals as used for the EXAFS measurement were used for single crystal analysis. The observed structure, $[(UO_2)_4(\mu_2\text{-}Cl)_4(\mu_3\text{-}O)_2(H_2O)_2(CH_3CN)_4]\cdot(CH_3CN)$, consists of a neutral tetrameric unit and one noncoordinating acetonitrile solvent molecule (Figure 8).

There are two crystallographic unique uranium sites present with pentagonal bipyramidal geometry; an inversion center of the centrosymmetric structure is located in the center of the tetramer. The $[(UO_2)_4(\mu_2\text{-}Cl)_4(\mu_3\text{-}O)_2(H_2O)_2(CH_3CN)_4]$ molecule is composed of four UO_2^{2+} ions linked

by two μ_3-oxygen atoms and four chloride bridges. In the equatorial plane, U1 is coordinated by two μ_2-bridging chloride anions (distance U1−Cl1 = 2.818(1) Å, U1−Cl2 = 2.824(1) Å), two μ_3-bridging oxo-ligands (distance U1−O5 = 2.231(3) Å, U1−O5[1−*x*,−*y*,2−*z*] = 2.252(4) Å), and one acetonitrile molecule (distance U1−N1 = 2.594(4) Å). U2 is in the equatorial plane surrounded by two μ_2-bridging chloride ions (distance U2−Cl1 = 2.817(1) Å, U2−Cl2[1−*x*,−*y*,2−*z*] = 2.788(1) Å), one μ_3-bridging oxo-ligand (distance U2−O5 = 2.218(4) Å), one acetonitrile molecule (distance U2−N2 = 2.555(4) Å), and one terminal bound water molecule (distance U2−O1 = 2.448(4) Å). The distances of U1 and U2 to the axial uranyl oxygen atoms, O_{ax}, range from 1.742(4) Å to 1.782(3) Å. The differences in the U−O_{ax} distances are also reflected by the unusually high Debye–Waller factor of 0.0055 Å^2 in the EXAFS spectrum. This value is usually below 0.0025 Å^2, even if the two axial oxygen atoms are not symmetry equivalent.[38] The Debye–Waller factor for the axial oxygen atoms observed for the solution species is 0.0014−0.0018 Å^2 (see Table 1), indicating a highly symmetrical arrangement. The two oxo-ligands O5 and O5[1−*x*,−*y*,2−*z*] are bound to U1, U1[1−*x*,−*y*,2−*z*], and U2 in a trigonal planar coordination, which distinguishes them clearly from hydroxyl groups that would exhibit a characteristic flattened trigonal pyramidal surrounding. The shortest U···U separation in the tetranuclear unit is found between U1 and U1[1−*x*,−*y*,2−*z*] and is 3.646 Å. This metal distance may already indicate a weak metal−metal interaction. The other U···U separations are U1−U2 = 3.963 Å, U1−U2[1−*x*,−*y*,2−*z*] = 3.952 Å, and U2−U2[1−*x*,−*y*,2−*z*] = 7.025 Å, respectively. The noncoordinating acetonitrile solvent molecule forms a hydrogen bond to the coordinated water molecules within a distance of O···N = 2.773(7) Å.

The strong tendency of uranyl to undergo a hydrolysis in aqueous solution is a known phenomenon that has been the subject of extensive studies.[39,40] The uranyl cation is acting as a strong Brønsted acid which results in the formation of uranyl hydroxides and protons. The hydrolysis has been described by the following equilibrium (1):

$$x{UO_2}^{2+} + yH_2O \leftrightarrow (UO_2)_x(OH)_y^{(2x-y)+} + yH^+ \qquad (1)$$

with *y* and *x* being the equivalents of uranyl and water molecules involved in the hydrolysis, respectively.[41,42] At near neutral pH values, the uranyl ion can create a number of polynuclear species.[43] A variety of uranyl tetramers with similar structure but absence of bridging chloride ligands has already been reported before.[44–46] Several U(VI) tetramers with a similar core coordination and bridging chloride atoms are known. Van den Bossche et al. reported on the chloride-bridged uranyl tetramer $[(UO_2)_4O_2Cl_4(C_4H_8O)_2(H_2O)_4]$ with tetrahydrofuran molecules coordinating to the two interior uranyl ions and two water molecules coordinating to each exterior UO_2^{2+} ion.[47] Gerasko et al. reported on a cucurbituril supramolecular compound with a $[(UO_2)_4O_2Cl_4(H_2O)_6]$ unit, which shows one water molecule coordinating for each interior uranyl ion and two water molecules coordinating to each exterior UO_2^{2+} ion.[48] The symmetry of the tetramer embedded in the supramolecule is higher than that of $[(UO_2)_4(\mu_2\text{-Cl})_4(\mu_3\text{-O})_2(H_2O)_2(CH_3CN)_4]\cdot(CH_3CN)$, which has two symmetry-independent bridging chloride atoms. The distances of the close-by uranyl ions in $[(UO_2)_4(\mu_2\text{-Cl})_4(\mu_3\text{-O})_2(H_2O)_2(CH_3CN)_4]$ are slightly shorter than those in the literature: U1−U1 = 3.646 Å compared with 3.682 Å (Van den Bossche et al.) and 3.668 Å (Gerasko et al.). Another U(VI) tetramer has been reported by Perrin et al.: the structure of $K_2(UO_2)_4O_2(OH)_2Cl_4(H_2O)_6$ consists of a core with only two bridging chlorides and two bridging hydroxides, whereas one additional chloride anion coordinates to each outer UO_2^{2+} ion.[49]

Additionally to the tendency of uranyl to undergo hydrolysis in aqueous solution, it has also been discussed in the literature that one of the characteristics of polar aprotic solvents is their ability to enormously enhance the basicity of anions as a consequence of an inefficient solvation of such species.[46] This proton redistribution may favor the formation and deposition of the described oxo-bridged species.

The coordination of the monomeric solution species $[UO_2Cl_2(H_2O)(MeCN)_2]$ partly undergoes a rearrangement during the formation of the tetrameric complex in the solid state. However, the coordination of two Cl^- atoms, one H_2O, and one MeCN molecule per uranium atom remains conserved. The comparison of the solution and the solid structure reveals significant differences. The U−Cl distance in solution (2.68 Å), where Cl^- is a free ligand, is shorter than in the crystal (2.82 Å), where Cl^- acts as bridging ligand. In the crystal structure, the distances to the coordinating solvent molecules becomes ∼0.02–0.04 Å longer than in the liquid, which is probably related with the stronger charge localization in the bridging oxo groups.

Acknowledgment. This work was supported by the Deutsche Forschungsgemeinschaft under Contract No. HE 2297/2-1. R.V.D. is a postdoctoral fellow of the K.U. Leuven Research Fund. R.V.D. acknowledges the financial support from the FWO-Vlaanderen ("Krediet aan Navorsers" project (No. 1.5.009.06)).

Supporting Information Available: CIF file for the crystal structure. This material is available free of charge via the Internet at http://pubs.acs.org.

IC7014435

(41) Lopez, M.; Birch, D. J. S. *Chem. Phys. Lett.* **1997**, *68*, 125.
(42) Wang, X.-F.; Andrews, L. *Inorg. Chem.* **2006**, *45*, 4157.
(43) Clark, D. L.; Conradson, S. D.; Donohoe, R. J.; Keogh, D. W.; Morris, D. E.; Palmer, P. D.; Rogers, R. D.; Tait, C. D. *Inorg. Chem.* **1999**, *38*, 1456.
(44) Borkowski, L. A.; Cahill, C. L. *Cryst. Growth Des.* **2006**, *6*, 2248.
(45) Crawford, M.-J.; Mayer, P.; Nöth, H.; Suter, M. *Inorg. Chem.* **2004**, *43*, 6860.
(46) Harrowfield, J. M.; Skelton, B. W.; White, A. H. *C. R. Chim.* **2005**, *8*, 169.
(47) Van den Bossche, G.; Spirlet, M. R.; Rebizant, J.; Goffart, J. *Acta Crystallogr.* **1987**, *C43*, 837.
(48) Gerasko, O. A.; Samsonenko, D. G.; Sharonova, A. A.; Virovets, A. V.; Lipkowski, J.; Fedin, V. P. *Russ. Chem. Bull.* **2002**, *51*, 346.
(49) Perrin, A.; Le Marouille, J. Y. *Acta Crystallogr.* **1977**, *B33*, 2477.